

Medial temporal lobe atrophy on MRI differentiates Alzheimer's disease from dementia with Lewy bodies and vascular cognitive impairment: a prospective study with pathological verification of diagnosis

E. J. Burton,¹ R. Barber,¹ E. B. Mukaetova-Ladinska,^{1,2} J. Robson,^{1,2} R. H. Perry,^{1,3,4}
E. Jaros,^{1,3,4,5} R. N. Kalaria^{1,6} and J. T. O'Brien¹

1 Institute for Ageing and Health, Newcastle University, Campus for Ageing and Vitality, UK

2 Research Neuropathology Laboratory, Newcastle University, Campus for Ageing and Vitality, UK

3 Department of Neuropathology, Newcastle Upon Tyne Hospitals NHS Trust, Newcastle General Hospital, UK

4 Cellular Pathology, Newcastle Upon Tyne Hospitals NHS Trust, Newcastle General Hospital, UK

5 Biomedical Research Centre, Newcastle University/NHS Partnership, UK

6 MRC Centre for Brain Ageing and Vitality, Newcastle University, Campus for Ageing and Vitality, UK

Correspondence to: Dr Emma J Burton,
Wolfson Research Centre, Institute for Ageing and Health,
Newcastle University, Campus for Ageing and Vitality,
Newcastle upon Tyne, NE4 5PL, UK
E-mail: e.j.burton@ncl.ac.uk

The purpose of this study was to determine the diagnostic accuracy of medial temporal lobe atrophy (MTA) on MRI for distinguishing Alzheimer's disease from other dementias in autopsy confirmed cases, and to determine pathological correlates of MTA in Alzheimer's disease, dementia with Lewy bodies (DLB) and vascular cognitive impairment (VCI). We studied 46 individuals who had both antemortem MRI and an autopsy. Subjects were clinicopathologically classified as having Alzheimer's disease ($n=11$), DLB ($n=23$) or VCI ($n=12$). MTA was rated visually using a standardized (Scheltens) scale blind to clinical or autopsy diagnosis. Neuropathological analysis included Braak staging as well as quantitative analysis of plaques, tangles and α -synuclein Lewy body-associated pathology in the hippocampus. Correlations between MTA and pathological measures were carried out using Spearman's rho, linear regression to assess the contributions of local pathologic changes to MTA. Receiver operator curve analysis was used to assess the diagnostic specificity of MTA for Alzheimer's disease among individuals with Alzheimer's disease, DLB and VCI. MTA was a highly accurate diagnostic marker for autopsy confirmed Alzheimer's disease (sensitivity of 91% and specificity of 94%) compared with DLB and VCI. Across the entire sample, correlations were observed between MTA and Braak stage ($\rho=0.50$, $P<0.001$), per cent area of plaques in the hippocampus ($\rho=0.37$, $P=0.014$) and per cent area of tangles in the hippocampus ($\rho=0.49$, $P=0.001$). Linear regression showed Braak stage ($P=0.022$) to be a significant predictor of MTA but not percent area of plaques ($P=0.375$), percent area of tangles ($P=0.330$) or percent area of Lewy bodies ($P=0.086$). MTA on MRI had robust discriminatory power for distinguishing Alzheimer's disease from DLB and VCI in pathologically confirmed cases. Pathologically, it is more strongly related to tangle rather than plaque or Lewy body pathology in the temporal lobe. It may have utility as a means for stratifying samples *in vivo* on the basis of putative differences in pathology.

Keywords: MTA; diagnosis; neuropathology

Abbreviations: CAMCOG = Cambridge Examination; DLB = dementia with Lewy bodies; MMSE = Mini-Mental State Exam; MTA = medial temporal lobe atrophy; NFT = neurofibrillary tangles; ROC = Receiver operator characteristic; VCI = vascular cognitive impairment

Introduction

Few studies have investigated the relationship between atrophy seen on MRI during life and the underlying neuropathological diagnosis of dementia. Such knowledge is essential to determine the specificity of imaging markers for one particular diagnosis or one type of pathology. In 13 Alzheimer's disease patients, Huesgen and colleagues (1993) found a correlation between a reduction in hippocampal volume and tangle but not plaque pathology. Similar findings at autopsy were reported from the Nun study (Gosche *et al.*, 2002), with hippocampal volume predicting differences in Braak stage in non-demented subjects. Others have found a correlation between MR volume reduction and hippocampal neuronal loss using post-mortem MRI (Bobinski *et al.*, 2000), though they did not report any associations with Alzheimer's disease pathology. A limited number of studies have examined antemortem MRI in relation to neuropathology. Jack and colleagues found a significant correlation between hippocampal volume reduction and Braak stage (tangle burden) in a group of 67 subjects with various dementia diagnoses including 23 with Alzheimer's disease. However, they did not examine links with plaques (Jack *et al.*, 2002).

These early studies suggest an association between volume loss, neuronal loss and tangle pathology but relied only on a rather crude measure of pathology, the 6-point Braak stage rather than more detailed quantification of pathology. A recent study reported correlations between antemortem hippocampal volumes and the density of neurofibrillary tangles (NFT) rather than the density of plaques in a small group of 10 Alzheimer's disease subjects compared with three non-demented controls (Csernansky *et al.*, 2004). Others found no correlation between the burden of beta amyloid and rates of brain atrophy or ventricular enlargement in demented and non-demented subjects, though correlations were observed between rates of atrophy and Braak stage (Josephs *et al.*, 2008). In a longitudinal study of 15 non-demented and 24 cognitively impaired subjects, the hippocampal volume measured prior to death was related to NFT burden rather than rate of hippocampal volume atrophy (Silbert *et al.*, 2003). However, specific hippocampal neuronal loss is likely to be the key substrate reflecting hippocampal volume changes in Alzheimer's disease (Zarow *et al.*, 2005).

Atrophy of the medial temporal lobe atrophy (MTA) is a well-recognized feature of Alzheimer's disease, though limitations regarding its specificity are increasingly being recognized as marked hippocampal atrophy has also been shown in fronto-temporal dementia (Galton *et al.*, 2001), dementia with Lewy bodies (DLB) (Barber *et al.*, 2000), Parkinson's disease with dementia (Tam *et al.*, 2005), vascular dementia (Barber *et al.*, 2000) and in very elderly people it is frequently associated with mixed pathology and hippocampal sclerosis in particular (Barkhof

et al., 2007). However, only one of these studies was in autopsy confirmed cases (Barkhof *et al.*, 2007) and thus misdiagnosis cannot be ruled out.

Galton *et al.* (2001) used a modified version of the widely recognized Scheltens scale (Scheltens *et al.*, 1992) to assess MTA and surrounding temporal lobe regions in Alzheimer's disease and semantic dementia. The group reported bilateral hippocampal atrophy in 50% of the Alzheimer's disease cases but interestingly demonstrated severe MTA in subjects with semantic dementia (Galton *et al.*, 2001). The same group also reported region of interest methods to correctly identify 75% of Alzheimer's disease cases (Galton *et al.*, 2001).

There is still some uncertainty with regard to the clinical value of MTA for the diagnosis of Alzheimer's disease. In recent years, studies looking at the specificity of MTA for Alzheimer's disease have shown results ranging from 50% (Galton *et al.*, 2001) to 96% (DeLeon *et al.*, 1997) in moderate to severe cases of Alzheimer's disease. In addition, the number of studies reporting hippocampal atrophy in subjects other than those with Alzheimer's disease is steadily increasing. Recent reports have shown MTA to be related to cognitive impairment in vascular dementia (Bastos-Leite *et al.*, 2007; Cho *et al.*, 2008) and therefore associated with pre-existing Alzheimer's disease. A study on subjects with amnesic cognitive impairment no dementia demonstrated global and temporal lobe atrophy which is suggestive of an increased risk of Alzheimer's disease (Jacova *et al.*, 2008). The findings raise important questions about the clinical utility of hippocampal atrophy on MRI as a diagnostic marker. Therefore determining the neuropathological changes that underlie hippocampal and MTA atrophy in different disorders is an important goal.

The primary aims of this study were to determine (i) the diagnostic accuracy of MTA for Alzheimer's disease in our autopsy confirmed cohort, and (ii) whether there was an association between MTA on MRI and neuropathological measures of plaques, NFTs and Lewy body-associated pathology in a cohort of neuropathologically confirmed cases.

Materials and Methods

Subjects

Subjects were selected from neuropathologically assessed cases in the Newcastle Brain Tissue Resource (NBTR). All subjects had originally been studied prospectively during life at the Institute for Ageing and Health, Newcastle University and underwent autopsy/brain donation at death. The subjects were part of longitudinal studies of dementia and post-stroke dementia and had undergone comprehensive annual clinical and cognitive assessments including CAMCOG (Cambridge Examination for Mental Disorders in the Elderly, Roth *et al.*, 1986) and MMSE (Mini-Mental State Exam, Folstein *et al.*, 1975) and had

had at least one MRI scan prior to death. They were recruited from hospital outpatients under the care of local old age psychiatrists, geriatricians and neurologists. Post-stroke patients were recruited from representative hospital-based stroke registers in Tyneside and Wearside. A diagnosis of Alzheimer's disease was in accordance to with National Institute of Neurologic and Communicative Disorders and Stroke/Alzheimer's Disease and Related Disorders (NINDS/ADRD) criteria for Alzheimer's disease (McKhann *et al.*, 1984). The consensus criteria for DLB and Parkinson's disease with dementia was used for a diagnosis of DLB (McKeith *et al.*, 1996) and the National Institute of Neurologic Disorders and Stroke/Association Internationale pour la Recherche et l'Enseignement en Neurosciences (NINDS/AIRENS) for a diagnosis of vascular dementia (Román *et al.*, 1993). The vascular dementia diagnosis was also consistent with the Harmonization Criteria for vascular cognitive impairment (VCI; Hachinski *et al.*, 2006). Stroke was defined using the World Health Organisation definition (WHO) and these subjects were cognitively assessed 3 months post-stroke. This study was approved by the local ethics committee of the Newcastle Hospitals Trusts Foundation. All subjects gave written informed consent for participation in the study and at death; their nearest relative gave permission for a post-mortem and subsequent use of autopsy material for research.

Subjects were selected on the basis of each having at least one MRI scan prior to autopsy and a diagnosis of Alzheimer's disease, DLB or VCI. We have used VCI and not vascular dementia because some subjects had cognitive impairment that fell short of dementia. A total of 52 subjects were identified. Of these, six were excluded because the MRI hard copy films had been destroyed. The study group consisted of 46 individuals who had both antemortem MRI and an autopsy. Subjects were pathologically classified as 11 AD, 23 DLB (nine of these had Parkinson's disease clinically for more than 1 year prior to the development of psychiatric features of DLB), and 12 VCI.

Clinical diagnoses at last assessment before death for these cases were as follows: For the DLB group 9 were clinically diagnosed as having Parkinson's disease with dementia and 15 as DLB. None of these cases changed following pathological confirmation and are grouped under DLB. All 12 cases in the VCI group were clinically and pathological matched (Kalaria *et al.*, 2004). Of the 11 pathological confirmed Alzheimer's disease cases 6 were Alzheimer's disease, 3 vascular dementia, 1 DLB and 1 stroke with dementia at the last clinical assessment. Of those with a change in diagnosis, four cases were clinically thought to be vascular but the predominant pathology was Alzheimer's disease, i.e. Braak stage >III and vascular pathology was largely restricted to microinfarcts (Kalaria *et al.*, 2004). The case clinically thought to be DLB had predominant Alzheimer's disease pathology in the form of tau positive neurofibrillary pathology and neuritic plaques compared with graded α -synuclein pathology (McKeith *et al.*, 2005).

Magnetic resonance imaging

Scan protocol 1

Twenty subjects had MRI scans performed on a 1.0T Siemens Magnetom Impact Expert MRI system (Siemens Medical, Erlangen, Germany). Whole brain T₁-weighted 3D MPRAGE (magnetization-prepared rapid-acquisition gradient echo) turbo flash datasets acquired in the sagittal plane (TR = 11.4 ms, TE = 4.4 ms, TI = 400 ms, 256 × 256 matrix, 1 mm slice thickness, cubic voxels of 1 mm, FOV = 256, flip angle 15°). Films for MTA rating.

Scan protocol 2

Twenty-six subjects had scans performed on a 1.5 Tesla GE Signa scanner (General Electric, Milwaukee, WI, USA). Whole brain T₁-weighted 3D FSPGR datasets were acquired in the coronal plane (TR = 12.4 ms, TE = 4.2 ms, TI = 650 ms, 256 × 256 matrix, 1.6 mm slice thickness, flip angle 15°, FOV = 20 cm, in plane resolution 0.78 × 0.78 mm).

MTA rating

A standardized scale (Scheltens scale) was used to rate right and left MTA from hard copies of T₁-weighted images (Scheltens *et al.*, 1992). Images from both scan protocols were printed in the coronal plane to permit MTA rating. The scale rates atrophy on a 5-point scale (0 = absent, 1 = minimal, 2 = mild, 3 = moderate and 4 = severe) based on the height of the hippocampal formation and the width of the CSF spaces. For the purpose of analysis the left and right scores were summed to give a combined MTA score (maximum score 8). All scans were assessed by consensus between two experienced raters (EJB and RB) blinded to diagnosis.

Neuropathological examination

Standard protocols for autopsy and brain removal were followed (Perry *et al.*, 1990; Perry *et al.*, 1996). As part of the neuropathological routine diagnostic assessment with in the Newcastle Brain Bank all subjects received standard macro brain examination of both cerebral hemispheres and microscopic examination of the right cerebral hemisphere including CERAD assessment for scoring of the density of neuritic plaques (Mirra *et al.*, 1991), Braak staging for NFT (Braak and Braak, 1991), Newcastle diagnostic criteria for Alzheimer's disease assessing mean neocortical tangle density (Perry *et al.*, 1996) and consensus cortical Lewy body staging for grading of α -synuclein pathology (McKeith *et al.*, 1996; McKeith *et al.*, 2005) and assessments of macro and microscopic vascular disease. In addition, we performed more detailed quantification of neuropathological features in the right archicortex, so that specific regional correlates could be made between antemortem MRI and neuropathology in the hippocampus.

Immunohistochemistry

Formalin-fixed paraffin blocks containing the temporal cortex and hippocampus (coronal levels 18/19, Perry *et al.*, 1996) were selected for the 46 cases. Twenty sections from each block were microtome sectioned at a thickness of 10 μ m and attached to silanized slides.

Sections were processed for immunohistochemistry in a standard manner (Lewis *et al.*, 2004). All slides were code numbered to ensure that analysis was carried out blind to diagnosis. Analysis was conducted on one section per anatomical area per subject. The sections were dewaxed with xylene and rehydrated. For α -synuclein and amyloid immunohistochemistry, the sections were incubated in 100% formic acid for 3 min and overnight, respectively, and then washed in distilled water for 5 min. For α -synuclein, to optimize antigen retrieval sections were subjected to pressure cooking in 1 mM EDTA (pH 8.0) for 2 min. Tau immunohistochemistry requires no pre-treatment. All sections were immersed in 3% hydrogen peroxide for 10 min; non-specific sites were blocked with 1% Marvel and incubated for 1 h at room temperature with the primary immunoprobes.

The primary antibodies used were: monoclonal mouse antibody (mAb) (6F/3D; used in 1:50 dilution, DAKO) directed against the

N-terminal portion of the amyloid protein, to demonstrate total density of β -amyloid plaques; mAb 1157 (an immunoprobe against the C-terminal end of tau protein used in 1:5 dilution, gift by Professor C.M. Wischick, University of Aberdeen) to visualize Alzheimer-type pathology including NFTs, dystrophic neurites and neuritic plaques; mAb NCL-ASYN (clone KM51, used in 1:30 dilution, Novocastra Laboratories Ltd, UK) to visualize Lewy body associated pathology, including α -synuclein-immunoreactive neuronal cytoplasmic inclusions and neurites. The slides were then thoroughly washed in PBS (50 mM TBS for amyloid immunohistochemistry) and incubated with biotinylated secondary antibody for 30 min at room temperature, followed by 30 min incubation with avidin HRP. All sections were finally washed under running tap water and the product visualized by 3'3' diaminobenzidine as the chromogen, counterstained with light haematoxylin, dehydrated, cleared and mounted. Brain tissue from two Alzheimer's disease, two DLB and two healthy elderly subjects were used to standardize each immunocytochemical run.

Neuropathology image acquisition in the hippocampus

Images were captured digitally at a magnification of $\times 10$ using a microscope (Nikon Eclipse) fitted with a motorized stage and coupled to a three-chip charge coupled device (CCD) colour video camera. Images were obtained from five areas of the hippocampus (molecular layer, CA1, CA2, CA3 and CA4). Each image had a captured surface area of 1.64 mm². Two images (3.28 mm²) were captured from each area, for each case and for each antibody.

Neuropathology quantification in the hippocampus

Quantification was carried out on a monitor using Image Pro Plus (version 4.0, Media Cybernetics, Silver Spring, MD, USA) in the hippocampus. A macro tool was developed to measure the burden of pathology (e.g. amyloid) expressed as a percentage of image area covered by immunoreactivity. This tool was designed based on the histogram of intensity threshold to calculate the percentage area of pathology (e.g. β -amyloid plaques, NFTs and Lewy body-associated neuronal cytoplasmic inclusions). Threshold levels could be manually adjusted by the user if it was necessary to include or exclude particular areas. For NFTs, neuronal cytoplasmic tangles were included in the assessment and neuropil and plaque neurites were excluded; for β -amyloid plaque assessments, plaque aggregates were included while vessels with amyloid angiopathy were excluded; for α -synuclein assessments, neuronal cytoplasmic inclusions were included while neuritic pathology was excluded.

Statistical analysis

The Statistical Package of Social Sciences (SPSS version 15, SPSS Inc., Chicago, IL) was used for data analysis. The Shapiro-Wilk test was used to examine normality of distribution of continuous variables for each group. Analysis of variance with post hoc Games-Howell was used for analysis of normally distributed data. For non-parametric data, Mann-Whitney U-test was used to look at differences between groups. Correlations between MTA scores, age and measures of neuropathology were examined using Spearman's rank order correlation coefficient. Linear regression was performed to find predictors of MTA. Variables entered into the regression for analysis were model 1—age at MRI; model 2—variable in model 1 and percentage

area of plaques, percentage area of tangles and Braak stage; and model 3—variables in model 2 and diagnosis of Alzheimer's disease. Receiver operator characteristic (ROC) analysis (Metz, 1978; Zweig and Campbell, 1993) was used to look at the sensitivity and specificity of MTA for Alzheimer's disease. For a given cut-off threshold the ROC curve shows the sensitivity and false-positive rate. All statistical tests were two-tailed and were regarded as significant at $P < 0.05$.

Results

Demographic details are summarized in Table 1. DLB subjects were younger than Alzheimer's disease ($P = 0.034$) and VCI ($P = 0.011$) subjects at death and at last MRI (Alzheimer's disease $P = 0.031$; VCI $P = 0.004$). Groups were comparable for gender ($\chi^2 = 0.518$, $df = 2$, $P = 0.77$). As expected, MMSE and CAMCOG scores were lower in subjects with Alzheimer's disease and DLB compared with VCI ($P = 0.001$). There were no significant differences between DLB and Alzheimer's disease.

Neuropathology and MTA differences

Visual rating of total MTA was greater for subjects with Alzheimer's disease than DLB and VCI ($P = 0.001$). There was no difference in total MTA scores between DLB and VCI ($P = 0.668$) (Table 2). Braak stage was significantly higher in subjects with Alzheimer's disease compared with DLB and VCI ($P = 0.001$). In general Alzheimer's disease subjects had greater percentage area of plaques and tangles than subjects with DLB (plaques $P = 0.002$; tangles $P = 0.003$) and VCI (plaques $P < 0.001$; tangles $P = 0.003$) (Table 2). There were no differences between DLB and VCI (plaques $P = 0.466$; tangles $P = 0.940$). As expected, DLB subjects had significantly greater percent area of Lewy body like pathology than Alzheimer's disease ($P = 0.001$) and VCI ($P < 0.001$). There were no differences between Alzheimer's disease and VCI ($P = 0.288$) (Table 2).

Relationship between MTA on MRI and pathology

Across the entire sample of 46 subjects, there were no correlations between Braak stage and age at death ($\rho = 0.135$, $P = 0.372$) or age at MRI ($\rho = 0.160$, $P = 0.484$). Total MTA correlated with both age at MRI ($\rho = 0.372$, $P = 0.011$) and age at death ($\rho = 0.362$, $P = 0.013$). Correlations were observed between total MTA and Braak stage ($\rho = 0.504$, $P < 0.001$, Fig. 1), percent area of β -amyloid plaques in the hippocampus ($\rho = 0.365$, $P = 0.014$), percent area of NFTs in the hippocampus ($\rho = 0.49$, $P < 0.001$) but not percent area of Lewy body-like inclusions in the hippocampus ($\rho = -0.185$, $P = 0.229$). As expected Braak stage correlated highly with measures of percent area of plaques ($\rho = 0.712$, $P < 0.001$) and tangles ($\rho = 0.668$, $P < 0.001$) but not Lewy body-like inclusions ($\rho = 0.107$, $P = 0.490$) (Table 3).

Regression

Linear regression analysis over the entire group showed Braak stage (NFT pathology) and age at death to be the only significant

Table 1 Subject characteristics

	Alzheimer's disease (n = 11)	DLB (n = 23)	VCI (n = 12)	P-value
Age at MRI (years)	81.93 ± 6.55	75.68 ± 6.43	82.69 ± 7.01	AD > DLB = 0.042 AD versus VCI NS VCI > DLB = 0.023
Age at death (years)	83.55 ± 6.69 (72.85–94.69)	77.22 ± 6.53 (64.10–91.43)	84.91 ± 6.91 (71.21–93.38)	AD > DLB = 0.044 AD versus VCI NS VCI > DLB = 0.012
Gender (M:F)	7:4	12:11	6:6	$\chi^2 = 0.5178$; $P = 0.772$
Postmortem delay (hours)	28.62 ± 19.21	48.95 ± 26.92	63.3 ± 18.49	AD versus DLB = 0.082 AD versus VCI = 0.004 DLB versus VCI = 0.201
Interval between MRI and death (years)	1.62 ± 1.09	1.53 ± 1.07	2.04 ± 1.51	NS
MMSE at MRI	13.8 ± 4.54	13.3 ± 7.83	22.83 ± 4.36	AD and DLB < VCI = 0.001 AD versus DLB NS
MMSE at last assessment	14.3 ± 4.37	9.56 ± 7.24	21.33 ± 5.17	AD < VCI = 0.007 DLB < VCI = 0.001 AD versus DLB NS
CAMCOG at MRI	50.8 ± 11.64	47.73 ± 23.37	76.25 ± 9.69	AD and DLB < VCI < 0.001 AD versus DLB NS
CAMCOG at last assessment	49.8 ± 12.86	42.0 ± 24.67	73.5 ± 16.04	AD < VCI = 0.003 DLB < VCI = 0.001 AD versus DLB NS

AD = Alzheimer's disease.

Table 2 Neuropathology and medial temporal lobe atrophy measures

	Alzheimer's disease (n = 11)	DLB (n = 23)	VCI (n = 12)	P-value
Braak staging (median, range)	5.36 ± 0.67 (5, 4–6)	3.17 ± 1.66 (3, 0–6)	2.83 ± 1.26 (2.5, 1–5)	AD > DLB and VCI = <0.001 DLB versus VCI NS
MTA visual rating right (median, range)	3.36 ± 0.92 (4, 1–4)	1.26 ± 1.09 (1, 0–4)	1.42 ± 0.90 (1.5, 0–3)	AD > DLB and VCI = <0.001 DLB versus VaD NS
MTA visual rating left (median, range)	3.45 ± 0.93 (4, 1–4)	1.26 ± 1.09 (1, 0–4)	1.25 ± 0.86 (1.5, 0–2)	AD > DLB and VCI = <0.001 DLB versus VCI NS
MTA visual rating total (median, range)	6.82 ± 1.77 (7, 2–8)	2.52 ± 2.11 (2, 0–8)	2.67 ± 1.72 (3, 0–5)	AD > DLB and VCI = <0.001 DLB versus VCI NS
Total Percentage area of plaques in hippocampus (range)	10.07 ± 10.93 (2.45–40.84)	3.21 ± 3.10 (0.03–10.81)	2.33 ± 3.53 (0.02–12.76)	AD versus DLB = 0.002 AD versus VCI = <0.001 DLB versus VCI NS
Total Percentage area of tangles in hippocampus (range)	6.34 ± 2.94 (1.59–12.89)	3.05 ± 3.41 (0.03–54.65)	2.57 ± 2.22 (0.16–7.72)	AD versus DLB = 0.003 AD versus VCI = 0.003 DLB versus VCI NS
Total Percentage area of Lewy body-associated pathology in hippocampus (range)	0.12 ± 0.103 (0.01–0.38)	1.51 ± 1.59 (0.01–5.43)	2.24 ± 0.488 (0.01–1.68)	AD versus DLB = 0.001 DLB versus VCI < 0.001 AD versus VCI = NS

VaD = vascular dementia. Values expressed as means ± SD unless otherwise stated. Median values are given for measures of MTA.

predictors of MTA (Table 4). In the first model age at death accounts for 16.9% of the variation in MTA, however when Braak stage is included (model 2) this increases to 39.6% of the variance with both age at death ($P = 0.018$) and Braak stage

($P = <0.001$) being significant contributors to the model. In model 3 with the addition of percent area of plaques, percent area of tangles and percent area of Lewy bodies in the hippocampus the variance increases slightly to 47.1%. In this model the

most significant contributor to MTA is Braak stage ($P=0.022$), with age at death no longer being significant ($P=0.106$). Percent areas of tangles, plaques and Lewy bodies make no significant contribution (tangles $P=0.330$; plaques $P=0.375$, Lewy bodies $P=0.084$). Although there was no significant difference in total MTA score between males and females ($P=0.971$), we repeated this regression analysis including gender as a predictor. The results obtained were similar to those in the original analysis but the inclusion of gender increased the significance effect of Braak stage ($P=0.003$) and age at death ($P=0.017$) on MTA.

MTA as a predictor of neuropathological diagnosis

The findings of the ROC analysis for the entire sample are presented in Fig. 2. The predictor is MTA and the predicted outcome is fulfilment of neuropathologic criteria for Alzheimer's disease compared with DLB and VCI. The area under the curve was 0.927 ($P<0.001$) with sensitivity and specificity values of 91% and 94% respectively for the best possible cut point of 5.5 (Fig. 2). Given that total MTA score cannot have a value of 0.5 we also calculated sensitivities and specificities based on two cut

points at ≥ 5 and ≥ 6 . For a cut point of ≥ 5 , the sensitivity was 83% and specificity as 95%. For the cut point of ≥ 6 , sensitivity was 71% and specificity as 95%.

Discussion

We observed significant differences in MTA, with Alzheimer's disease subjects showing more hippocampal atrophy than subjects with DLB or VCI, as would be expected and has previously been reported (Scheltens *et al.*, 1992; Jack *et al.*, 1997; Barber *et al.*, 1999). This is in accord with later studies too. Jack *et al.* (2002) found smaller antemortem hippocampal volumes in Alzheimer's disease compared to non-demented subjects. However the group did report small hippocampi were found in other causes of dementia not just Alzheimer's disease. In addition Gosche *et al.* (2002) found post-mortem hippocampal volume on MRI was a better predictor of Alzheimer's disease neuropathology than clinical diagnosis or measures of cognition. In contrast, others have reported that hippocampal atrophy was not specific for Alzheimer's disease pathology, however in these studies the subjects' classification was based on clinical rather than pathological assessments (Laakso *et al.*, 1996; Riekkinen *et al.*, 1998).

Using postmortem MRI in the oldest old, Barkhof and colleagues reported high MTA scores (greater hippocampal atrophy) to be associated with significant Alzheimer's disease pathology though the authors reported a lack of discriminative potential of MTA in post-mortem MRI ratings (Barkhof *et al.*, 2007). However

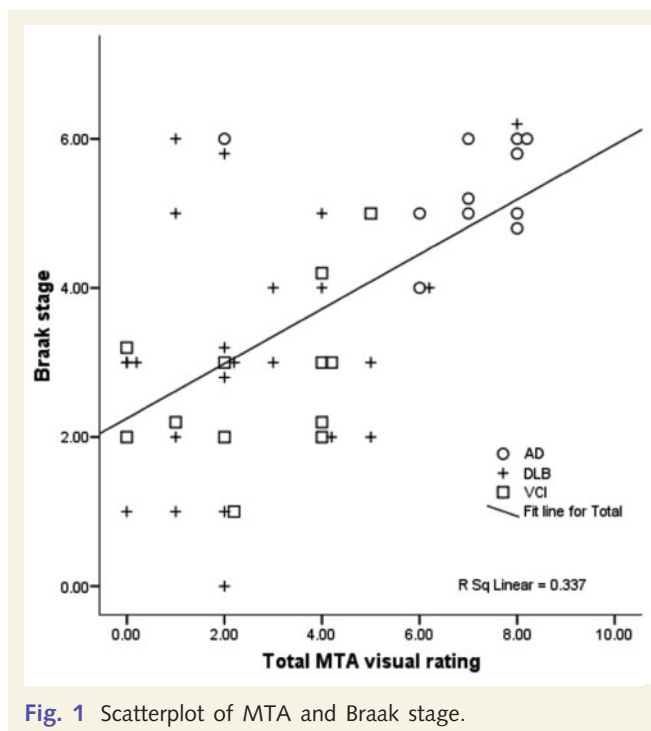


Fig. 1 Scatterplot of MTA and Braak stage.

Table 4 Results of the regression analysis

	R ² (% variance)	β value	P-value
Model 1			
Age at death	0.169 (16.9%)	0.411	0.006
Model 2			
Age at death	0.396 (39.6%)	0.307	0.018
Braak stage		0.488	<0.001
Model 3			
Age at death	0.471 (47.1%)	0.216	0.106
Braak stage		0.376	0.022
Area plaques in hippocampus (%)		0.127	0.375
Area tangles in hippocampus (%)		0.161	0.330
Area LB-like pathology in hippocampus (%)		-0.229	0.084

Table 3 Correlations between antemortem MTA rating on MRI and neuropathology variables in the hippocampus

	Braak stage	Area β -amyloid plaques (%)	Area of neurofibrillary tangles (%)	Area of Lewy body-associated pathology (%)
MTA rating (right)	0.458 ($P<0.001$)	0.381 ($P=0.010$)	0.507 ($P<0.001$)	-0.224 ($P=0.143$)
MTA rating (left)	0.544 ($P<0.001$)	0.339 ($P=0.023$)	0.468 ($P=0.001$)	-0.137 ($P=0.377$)
MTA rating (total)	0.504 ($P<0.001$)	0.365 ($P=0.014$)	0.486 ($P=0.001$)	-0.185 ($P=0.229$)

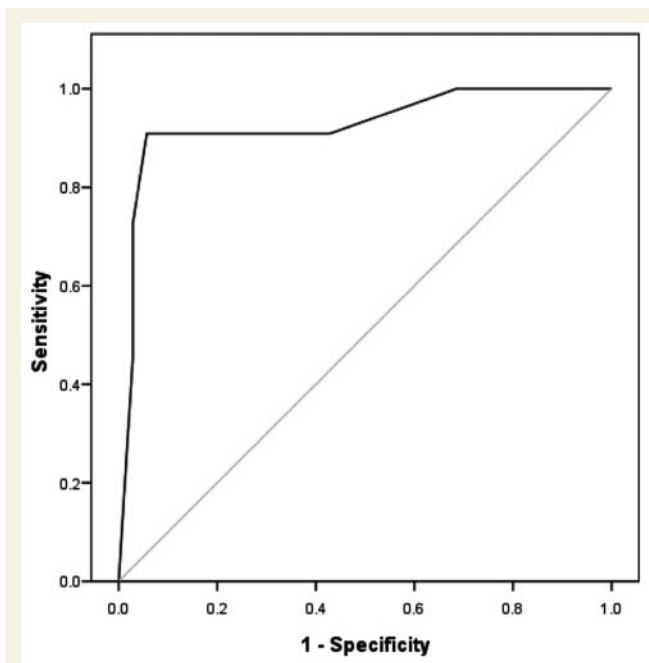


Fig. 2 ROC curve for medial temporal lobe atrophy using a diagnosis of Alzheimer's disease as the classification variable. The grey line is the cutoff reference line.

we found MTA to be a highly accurate diagnostic marker for autopsy confirmed Alzheimer's disease (sensitivity 91% and a specificity of 94%) using ROC analysis in this sample with a mean age of 80.7 years.

Consistent with the association of a diagnosis of Alzheimer's disease, we found MTA on MRI to correlate with NFT pathology (Braak stage and per cent area of NFTs) in a group of autopsy confirmed cases. This finding concurs with other studies that have found significant correlations between Braak stage and hippocampal volume in non-demented subjects (Gosche *et al.*, 2002) and subjects with various forms of dementia including Alzheimer's disease (Jack *et al.*, 2002). These studies looked at the association of brain atrophy and tangle pathology (Braak stage) but did not examine links with β -amyloid plaques and also relied on the relatively crude semi-quantitative grading of pathology (relying on the six point Braak staging). In contrast, we quantified the neuropathological changes by measuring the percent area covered by plaques, tangles and Lewy body-associated pathology to give a more representative burden of pathology than the widely used Braak stage. We report strong correlations between hippocampal atrophy and the percent area of β -amyloid plaques and NFTs but not Lewy body-associated neuronal inclusions. Reassuringly our methods of quantification also correlate with the Braak staging. Figure 1 also demonstrates that most DLB cases with high Braak scores (five or six) do not show the degree of MRI hippocampal atrophy found in Alzheimer's disease cases, possibly indicating differing mechanisms of tau pathology acquisition with different consequences for neuronal and/or neuropil loss in the two diseases.

Previous studies have shown neuronal loss and volume reduction in CA1 subfield of the hippocampus to be correlated with

dementia severity (Bobinski *et al.*, 1998; Price *et al.*, 2001; Zarow *et al.*, 2005). Csernansky *et al.* (2004) found that the density of NFT in CA1 hippocampal subfield rather than senile plaques density correlated with hippocampal volume, while total cerebral volume better correlated with hippocampal senile plaques density than NFT density.

Our study in pathologically confirmed cases provides further support to the already established body of literature that show MTA to be significant in Alzheimer's disease. We acknowledge that although the results of our study show high diagnostic accuracy of MTA for Alzheimer's disease, this may not apply widely and must be taken in the context of previously published data. Galton *et al.* (2001) used a modified version of the widely used Scheltens scale and incorporated other non-hippocampal structures in their assessment of MTA. They compared Alzheimer's disease and frontotemporal dementia cases reporting that only 50% of Alzheimer's disease patients had bilateral MTA. In contrast other studies using the same visual rating scale as we have employed, showed MTA atrophy in a higher percentage of Alzheimer's disease patients. Scheltens *et al.* found 81% of their severe Alzheimer's disease cases had MTA. This is supported by others in studies of mild (84%, DeLeon *et al.*, 1997) and moderate Alzheimer's disease (93%, O'Brien *et al.*, 1994; 96% DeLeon *et al.*, 1997). However, our sample is unique in that the cases were prospectively assessed over 10 years and all had neuropathological confirmation of diagnosis which contrasts with the majority of previous studies.

Potential limitations of the study include the interval between MRI and death in the present study. The average of 1.5 years was recorded in the DLB group, 1.6 years in the Alzheimer's disease group and 2 years in the VCI group. These are similar if not shorter than in other studies where intervals of up to 3 years have been reported (Jagust *et al.*, 2008). Even with a relatively short time interval we must consider that this delay may underestimate the degree of MTA seen on MR in our cases.

The use of a visual rating scale rather than region of interest volumetric measure to assess MTA (Scheltens *et al.*, 1992) is another possible limitation of the study. This scale which rates the height of the hippocampus and the width of the surrounding CSF spaces is easily applied in a clinical setting and has shown good diagnostic performance *in vivo* (Scheltens *et al.*, 1992; O'Brien *et al.*, 1994). In comparison, region of interest or volumetric measurements tend to be more accurate but require some degree of training, greater time and effort and may not be easily transferable to a clinical setting where it would be of most value. Antemortem brain structure shown on MR may become useful in combination with clinical assessments to improve the monitoring of disease severity in Alzheimer's disease patients.

Unlike recent studies, we only used cross-sectional data obtained from the MRI scans taken close to death. Tracking atrophy over time using serial MRI scans could be important although the results may not always be enlightening. Silbert *et al.* (2003) described correlations between rates of ventricular enlargement and amyloid deposition but found no association between rates of brain atrophy and senile plaques density. However, rates of cerebral atrophy were related to NFT pathology. They also found the rate of ventricular CSF volume was the best predictor

of cortical NFT and senile plaques. Interestingly, the rate of hippocampal volume loss was not a valid predictor of the degree of hippocampal NFT pathology (Silbert *et al.*, 2003). By contrast, Josephs *et al.* (2008) recently showed that atrophy overtime was not associated with amyloid burden but did report a correlation between Braak stage and rates of atrophy. Other studies support the notion that progressive brain tissue loss (Whitwell *et al.*, 2007) is more likely to be associated with tangle burden, i.e. Braak staging rather than with plaque pathology (Nagy *et al.*, 1996).

Conclusion

Our findings of an association between hippocampal atrophy and measures of Alzheimer's disease pathology (plaques and tangles) agree with other imaging correlation studies. MTA has excellent discriminatory power for Alzheimer's disease compared to DLB and VCI in pathologically confirmed cases. Pathological correlates of MTA include both senile plaques and NFT, but not Lewy body-associated pathology, with the major contributor being Braak stage (NFT pathology). Further studies are needed as this may not apply in all situations for example distinguishing Alzheimer's disease from frontotemporal dementia where MTA atrophy may be of similar severity.

Acknowledgements

We thank the Alzheimer's Research Trust (ART), PPP foundation and Alzheimer's Society (London) for financial support. We also thank the neuropathology staff. Dr Burton holds an ART fellowship.

Funding

Medical Research Council (to NBTR, partial). Our work is also supported by a programme grant on vascular factors in dementia and neurodegeneration from the MRC.

References

- Barber R, Ballard C, McKeith IG, Gholkar A, O'Brien JT. MRI volumetric study of dementia with Lewy bodies: a comparison with AD and vascular dementia. *Neurology* 2000; 54: 1304–9.
- Barber R, Gholkar A, Scheltens P, Ballard C, McKeith IG, Morris CM, et al. Apolipoprotein E epsilon4 allele, temporal lobe atrophy and white matter lesions in late-life dementia. *Arch Neurol* 1999; 56: 961–6.
- Barkhof F, Polvikoski TM, van Straaten ECW, Kalaria RN, Sulkava R, Aronen HJ, et al. The significance of medial temporal lobe atrophy: a post-mortem MRI study in the very old. *Neurology* 2007; 69: 1521–27.
- Bobinski M, de Leon MJ, Tarnawski M, Wegiel J, Reisberg B, Miller DC, et al. Neuronal and volume loss in CA1 of the hippocampal formation uniquely predicts duration and severity of Alzheimer's disease. *Brain Res* 1998; 805: 267–9.
- Bobinski M, de Leon MJ, Wegiel J, Desanti S, Convit A, Saint Louis LA, et al. The histological validation of post mortem magnetic resonance imaging-determined hippocampal volumes in Alzheimer's disease. *Neuroscience* 2000; 95: 721–5.
- Braak H, Braak E. Neuropathological staging of Alzheimer-related changes. *Acta Neuropathol* 1991; 82: 239–59.
- Csernansky JG, Hamstra J, Wang L, McKeel D, Price JL, Gado M, et al. Correlations between antemortem hippocampal volume and post-mortem neuropathology in AD subjects. *Alzheimer Dis Assoc Disord* 2004; 18: 190–5.
- Folstein MF, Folstein SE, McHugh PR. "Mini-mental state". A practical method for grading the cognitive state of patients for the clinician. *J Psychiatr Res* 1975; 12: 189–98.
- Galton CJ, Patterson K, Graham K, Lambon-Ralph MA, Williams G, Antoun N, et al. Differing patterns of temporal atrophy in Alzheimer's disease and semantic dementia. *Neurology* 2001; 57: 216–25.
- Gosche KM, Mortimer JA, Smith CD, Markesbery WR, Snowdon DA. Hippocampal volume as an index of Alzheimer neuropathology: findings from the Nun study. *Neurology* 2002; 58: 1476–82.
- Hachinski V, Iadecola C, Petersen RC, Breteler MM, Nyenhuis DL, Black SE, et al. National institute of neurological disorders and stroke—Canadian stroke network vascular cognitive impairment harmonization standards. *Stroke* 2006; 37: 2220–41.
- Huesgen CT, Burger PC, Crain BJ, Johnson GA. In vitro MR microscopy of the hippocampus in Alzheimer's disease. *Neurology* 1993; 43: 145–52.
- Jack CR Jr, Dickson DW, Parisi JE, Xu YC, Cha RH, O'Brien PC, et al. Antemortem MRI findings correlate with hippocampal neuropathology in typical aging and dementia. *Neurology* 2002; 8: 750–7.
- Jack CR Jr, Petersen RC, Xu YC, Waring SC, O'Brien PC, Tangalos EG, et al. Medial temporal lobe atrophy on MRI in normal aging and very mild Alzheimer's disease. *Neurology* 1997; 49: 786–94.
- Jagust WJ, Zheng L, Harvey DJ, Mack WJ, Vinters HV, Weiner MW, et al. Neuropathological basis of magnetic resonance images in aging and dementia. *Ann Neurol* 2008; 63: 72–80.
- Josephs KA, Whitwell JL, Ahmed Z, Shiung MM, Weigand SD, Knopman DS, et al. β -Amyloid burden is not associated with rates of brain atrophy. *Ann Neurol* 2008; 63: 204–12.
- Kalaria RN, Kenny RA, Ballard CG, Perry R, Ince P, Polvikoski T. Towards defining the neuropathological substrates of vascular dementia. *J Neuro Sci* 2004; 226: 75–80.
- Kril JJ, Hodges J, Halliday G. Relationship between hippocampal volume and CA1 neuron loss in brains of humans with and without Alzheimer's disease. *Neurosci Lett* 2004; 361: 9–12.
- Laakso MP, Partanen K, Riekkinen P, Lehtovirta M, Helkala EL, Hallikainen M, et al. Hippocampal volumes in Alzheimer's disease, Parkinson's disease with and without dementia, and in vascular dementia: An MRI study. *Neurology* 1996; 46: 678–81.
- Lewis H, Behr D, Cookson N, Oakley A, Piggott M, Morris CM, et al. Quantification of Alzheimer pathology in ageing and dementia: age-related accumulation of amyloid-beta(42) peptide in vascular dementia. *Neuropathol Appl Neurobiol* 2006; 32: 103–18.
- McKeith IG, Dickinson DW, Lowe J, Emre M, O'Brien JT, Feldman H, et al. Diagnosis and management of dementia with Lewy bodies: third report of the DLB Consortium. *Neurology* 2005; 65: 1863–72.
- McKeith IG, Galasko D, Kosaka K, Perry EK, Dickson DW, Hansen LA, et al. Consensus guidelines for the clinical and pathological diagnosis of dementia with Lewy bodies (DLB): report of the consortium on DLB international workshop. *Neurology* 1996; 47: 1113–24.
- McKhann G, Drachman D, Folstein M, Katzman R, Price D, Stadlan EM. Clinical diagnosis of Alzheimer's disease: report of the NINCDS-ADRDA Work Group under the auspices of Department of Health and Human Services Task Force on Alzheimer's Disease. *Neurology* 1984; 34: 939–44.
- Metz CE. Basic principles of ROC analysis. *Semin Nucl Med* 1978; 8: 283–98.
- Mirra SS, Heyman A, McKeel D, Sumi SM, Crain BJ, Brownlee LM, et al. The consortium to establish a registry for Alzheimer's disease (CERAD). Part II. Standardization of the neuropathologic assessment of Alzheimer's disease. *Neurology* 1991; 41: 479–86.

- Nagy Z, Jobst KA, Essiri MM, Morris JH, King EM, MacDonald B, et al. Hippocampal pathology reflects memory deficit and brain imaging measurements in Alzheimer's disease: clinicopathologic correlations using three sets of pathologic diagnostic criteria. *Dementia* 1996; 7: 76–81.
- Perry RH, Irving D, Blessed G, Fairbairn A, Perry EK. Senile dementia of Lewy body type. A clinically and neuropathologically distinct form of Lewy body dementia in the elderly. *J Neurol Sci* 1990; 95: 119–39.
- Perry RH, Jaros EB, Irving D, Scoones DL, Brown A, McMeekin WM, et al. What is the neuropathological basis of dementia associated with Lewy Bodies. In: Perry RH, McKeith IG, Perry EK, editors. *Dementia with lewy bodies*. Cambridge: Cambridge University Press; 1996. p. 212–23.
- Price JL, Ko AI, Wade MJ, Tsou SK, McKeel DW, Morris JC. Neuron number in the entorhinal cortex and CA1 in preclinical Alzheimer disease. *Arch Neurol* 2001; 58: 1395–402.
- Riekkinen P Jr, Kejonen K, Laakso MP, Soininen H, Partanen K, Riekkinen M. Hippocampal atrophy is related to impaired memory, but not frontal functions in non-demented Parkinson's disease patients. *Neuroreport* 1998; 9: 1507–11.
- Román GC, Tatemichi TK, Erkinjuntti T, Cummings JL, Masdeu JC, Garcia JH, et al. Vascular dementia: diagnostic criteria for research studies. Report of the NINDS-AIREN International Workshop. *Neurology* 1993; 43: 250–60.
- Roth M, Tym E, Mountjoy CQ, Huppert FA, Hendrie H, Verma S, et al. Camdex. A standardised instrument for the diagnosis of mental disorder in the elderly with special reference to the early detection of dementia. *Br J Psychiatry* 1986; 149: 698–709.
- Scheltens P, Fox N, Barkhof F, De Carli C. Structural magnetic resonance imaging in the practical assessment of dementia: beyond exclusion. *Lancet Neurol* 2002; 1: 13–21.
- Scheltens P, Leys D, Barkhof F, De Carli C. Atrophy of medial temporal lobes on MRI in 'probable' Alzheimer's disease and normal ageing: diagnostic value and neuropsychological correlates. *J Neurol Neurosurg Psychiatry* 1992; 55: 967–72.
- Silbert LC, Quinn JF, Moore MM, Corbridge E, Ball MJ, Murdoch G, et al. Changes in premorbid brain volume predict Alzheimer's disease pathology. *Neurology* 2003; 61: 487–92.
- Tam CWC, Burton EJ, McKeith IG, Burn DJ, O'Brien JT. Temporal lobe atrophy on MRI in Parkinson's disease with dementia: a comparison with Alzheimer's disease and dementia with Lewy bodies. *Neurology* 2005; 64: 861–5.
- Whitwell JL, Przybelski SA, Weigand SD, Knopman DS, Boeve BF, Petersen RC, et al. 3D maps from multiple MRI illustrate changing atrophy patterns as subjects progress from mild cognitive impairment to Alzheimer's disease. *Brain* 2007; 130: 1777–86.
- World Health Organisation, MONICA project principal investigators. The world health organisation MONICA project (monitoring trends and determinants in cardiovascular disease): a major international collaboration. *J Clin Epidemiol* 1988; 41: 105–14.
- Zarow C, Vinters HV, Ellis WG, Weiner MW, Mungas D, White L, et al. Correlates of hippocampal neuron number in Alzheimer's disease and ischemic vascular dementia. *Ann Neurol* 2005; 57: 896–903.
- Zweig MH, Campbell G. Receiver operating characteristic (ROC) plots—A fundamental evaluation tool in Clinical medicine. *Clin Chem* 1993; 39: 561–77. (Erratum *Clin Chem*. 1993; 39: 1589).